Articles

Reactive Deposition of Conformal Ruthenium Films from Supercritical Carbon Dioxide

Adam O'Neil and James J. Watkins*

Departments of Chemical Engineering and Polymer Science and Engineering, University of Massachusetts, Amherst, Massachusetts 01003

Received January 19, 2006. Revised Manuscript Received July 11, 2006

High-purity Ru films were deposited from supercritical carbon dioxide onto the native oxide of Si wafers and onto Ta films supported on Si wafers using a batch, cold wall deposition reactor. Ru(0) and Ru(II) precursors were effective at substrate temperatures between 175 and 300 °C and pressures between 20 and 25 MPa. Hydrogen-assisted deposition of Ru from triruthenium dodecacarbonyl ($Ru_3(CO)_{12}$), tris(2,2,6,6-tetramethyl-heptane-3,5-dionato)ruthenium ($Ru(tmhd)_3$), and bis(2,2,6,6-tetramethyl heptane-3,5-dionato)(1,5-cyclooctadiene)ruthenium ($Ru(tmhd)_2cod$) proceeded readily to yield highly reflective thin films with resistivities as low as 22 $\mu\Omega$-cm for a 33 nm thick film. H_2-assisted depositions using ruthenocene were not successful on oxide surfaces at temperatures up to 300 °C, but proceeded readily on Au. Thermal depositions from ($Ru_3(CO)_{12}$) yielded reflective, but highly resistive, films. Excellent step coverage of high-purity films was achieved within 200 nm × 300 nm trenches on patterned tantalum-coated surfaces and within 2 μm × 30 μm and 300 nm × 1.2 μm via structures on etched silicon wafers by H_2-assisted deposition using $Ru_3(CO)_{12}$ and $Ru(tmhd)_2cod$, respectively. Analysis by X-ray diffraction and X-ray photoelectron spectroscopy indicated that the films were polycrystalline and free of oxygen contamination.

Introduction

The preparation of conformal Ru films is of broad interest for applications in microelectronics including electrodes for dynamic random access memory (DRAM), nonvolatile ferroelectric memory (FeRAM), and potentially as conducting diffusion barriers in Cu interconnect structures for integrated circuits. Each of these applications requires conformal step coverage in high aspect ratio features. Additional integration requirements include low deposition temperatures (<400 °C) for Cu interconnects, high film purity, control of surface morphology, and acceptable adhesion. In the case of Cu diffusion barriers film thicknesses below 5 nm are required.[1] The deposition of continuous, low-resistivity diffusion barriers (Ru resistivity = 7.6 $\mu\Omega$-cm at 0 °C) would enable direct electrodeposition of Cu onto the barrier without the need for an additional seed layer.[2]

Reactive deposition of Ru has traditionally been carried out by chemical vapor deposition (CVD) or atomic layer deposition (ALD). While CVD has been used to deposit films of both Ru and RuO_2, the identification of suitable ruthenium precursors, acceptable process methodologies, and film quality remain significant issues. The precursor systems studied to date have been almost exclusively based on cyclopentadiene[3−5] (or ethyl derivatives[6−12]), carbonyl,[13−16] β-diketonate[17−29] ligands, or combinations of various mixed ligand systems.[30−36] Work has also been carried out using highly toxic RuO_4 species.[37,38] Typically, CVD depositions

(1) International Technology Roadmap for Semiconductors (ITRS); http://public.itrs.net/Files/2003ITRS/Home2003.htm, 2003.
(2) Chan, R.; Arunagiri, T. N.; Zhang, Y.; Chyan, O.; Wallace, R. M.; Kim, M. J.; Hurd, T. Q. *Electrochem. Solid State Lett.* **2004**, *7*, G154−G157.
(3) Park, S. E.; Kim, H. M.; Kim, K. B.; Min, S. H. *J. Electrochem. Soc.* **2000**, *147*, 203−209.
(4) Aoyama, T.; Kiyotoshi, M.; Yamazaki, S.; Eguchi, K. *Jpn. J. Appl. Phys., Part 1* **1999**, *38*, 2194−2199.
(5) Trent, D. E.; Paris, B.; Krause, H. H. *Inorg. Chem.* **1964**, *3*, 1057−1058.
(6) Kim, J. J.; Jung, D. H.; Kim, M. S.; Kim, S. H.; Yoon, D. Y. *Thin Solid Films* **2002**, *409*, 28−32.
(7) Aoyama, T.; Eguchi, K. *Jpn. J. Appl. Phys., Part 2* **1999**, *38*, L1134−L1136.
(8) Matsui, Y.; Hiratani, M.; Nabatame, T.; Shimamoto, Y.; Kimura, S. *Electrochem. Solid State Lett.* **2001**, *4*, C9−C12.
(9) Matsui, Y.; Hiratani, M.; Nabatame, T.; Shimamoto, Y.; Kimura, S. *Electrochem. Solid State Lett.* **2002**, *5*, C18−C21.
(10) Nabatame, T.; Hiratani, M.; Kadoshima, M.; Shimamoto, Y.; Matsui, Y.; Ohji, Y.; Asano, I.; Fujiwara, T.; Suzuki, T. *Jpn. J. Appl. Phys., Part 2* **2000**, *39*, L1188−L1190.
(11) Jin, X.; Wade, C. P.; Tao, X.; Pao, E.; Wang, Y.; Zhao, J. U.S. Patent 6479100, 2002.
(12) Wade, C. P.; Pao, E.; Wang, Y.; Zhao, J. U.S. Patent 6440495, 2002.
(13) Berry, A. D.; Brown, D. J.; Kaplan, R.; Cukauskas, E. J. *J. Vac. Sci. Technol., A* **1986**, *4*, 215−218.
(14) Boyd, E. P.; Ketchum, D. R.; Deng, H. B.; Shore, S. G. *Chem. Mater.* **1997**, *9*, 1154−1158.
(15) Wang, Q.; Ekerdt, J. G.; Gay, D.; Sun, Y. M.; White, J. M. *Appl. Phys. Lett.* **2004**, *84*, 1380−1382.
(16) Lee, F. J.; Chi, Y.; Liu, C. S.; Hsu, P. F.; Chou, T. Y.; Peng, S. M.; Lee, G. H. *Chem. Vap. Dep.* **2001**, *7*, 99−101.
(17) Crosby, J. N.; Hanley, R. S. U.S. Patent 4250210, 1981.
(18) Lee, D. J.; Kang, S. W.; Rhee, S. W. *Thin Solid Films* **2002**, *413*, 237−242.

10.1021/cm060142d CCC: $33.50 © 2006 American Chemical Society
Published on Web 10/27/2006

employ an oxidizing environment, which can prove to be problematic for some substrates such as Ta[39] and can lead to unacceptable levels of oxygen contamination in the film. Film purity has also been an issue due to carbon contamination from ligand decomposition products. Wang et al. recently demonstrated thermal deposition from $Ru_3(CO)_{12}$ onto Ta via CVD; however, uniform, conformal film deposition over large areas remains elusive.[15]

The need for continuous and conformal ultrathin (~5 nm) Ru films for use as Cu diffusion barriers and adhesion promotion layers for interconnect structures in integrated circuits has prompted investigations of Ru depositions by ALD. For example, films have been grown using alternating pulses of $Ru(tmhd)_2$cod or bis(ethylcyclopentadienyl)ruthenium and oxygen.[40,41] While ALD can yield good step coverage and high purity, the deposition rate is too slow for many applications, including electrode deposition. Also, as noted above, the use of O_2 as a reactant gas can be problematic for some substrates.

In this paper we report the hydrogen-assisted deposition of high-purity, conformal Ru films onto the native oxide of Si wafers and onto Ta via supercritical fluid deposition (SFD). SFD is essentially a hybrid approach to reactive metal deposition that combines the advantages of solution-based processes, namely, high precursor concentration and the elimination of precursor volatility constraints, with those of vapor-phase techniques, namely, favorable transport properties and the absence of surface tension. We and others have demonstrated the utility of SFD for the deposition of Au, Cu, Co, Ni, Ir, Rh, Pd, and Pt films with exceptional step coverage.[42−54] A detailed study of Cu deposition from supercritical CO_2 revealed that high precursor concentrations can yield zero-order, surface reaction rate-limited kinetics that promote conformal deposition.[54] Moreover, most metal depositions utilizing SFD can be carried out in a cold wall reactor in which deposition is selective for the heated substrate while competing deposition on the reactor walls and gas-phase nucleation can be eliminated. Depositions are carried out at lower temperatures than equivalent CVD experiments, which minimize ligand fragmentation that can result in film contamination.

We find that H_2-assisted deposition using dodecacarbonyl triruthenium ($Ru_3(CO)_{12}$), tris(2,2,6,6-tetramethyl-heptane-3,5-dionato)ruthenium ($Ru(tmhd)_3$, or bis(2,2,6,6-tetramethyl heptane-3,5-dionato)(1,5-cyclooctadiene)ruthenium ($Ru(tmhd)_2$cod) yields high-quality Ru films directly on the native oxide of Si wafers and on Ta films supported on Si wafers. H_2-assisted depositions on these substrates using ruthenocence were not successful; however, depositions using this precursor on wafers seeded with Au yielded Ru films. This result is in agreement with the results of Kondoh, who reported that Ru film growth from SCF CO_2 onto patterned wafers required coating the wafers with gold.[53] We show that this is not the case for other precursors.

Successful deposition of pure Ru films using a reducing atmosphere rather than via oxidation represents a departure from typical CVD strategies and offers compelling advantages for minimizing oxygen incorporation in the film and for use with substrates that are susceptible to spontaneous oxidation. Moreover, we demonstrate excellent step coverage of high aspect ratio (2 μm × 30 μm) features, which is relevant to the deposition of electrodes in capacitor structures.

Experimental Section

Ruthenocene ($Ru(Cp)_2$, 99%), dicarbonyl cyclopentadienyl ruthenium ($[Ru(CO)_2Cp]_2$, 99%), dodecacarbonyl triruthenium (Ru_3-

(19) Lee, J. H.; Kim, J. Y.; Rhee, S. W.; Yang, D. Y.; Kim, D. H.; Yang, C. H.; Han, Y. K.; Hwang, C. J. *J. Vac. Sci. Technol., A* **2000**, *18*, 2400−2403.
(20) Lee, J. M.; Kang, S. Y.; Shin, J. C.; Hwang, C. S.; Kim, H. J.; Suk, C. G. *J. Korean Phys. Soc.* **1999**, *35*, S107−S109.
(21) Lee, J. W.; Kim, K. M.; Song, H. S.; Jeong, K. C.; Lee, J. M.; Roh, J. S. *Jpn. J. Appl. Phys., Part 1* **2001**, *40*, 5201−5205.
(22) Lee, S. H.; Chun, J. K.; Hur, J. J.; Lee, J. S.; Rue, G. H.; Bae, Y. H.; Hahm, S. H.; Lee, Y. H.; Lee, J. H. *IEEE Electron Device Lett.* **2000**, *21*, 261−263.
(23) Kadoshima, M.; Nabatame, T.; Hiratani, M.; Nakamura, Y.; Asano, I.; Suzuki, T. *Jpn. J. Appl. Phys., Part 2* **2002**, *41*, L347−L350.
(24) Kim, Y.; Ha, S. C.; Jeong, K. C.; Hong, K.; Roh, J. S.; Yoon, H. K. *Integr. Ferroelectr.* **2001**, *36*, 285−294.
(25) Kim, K. W.; Kim, N. S.; Kim, Y. S.; Choi, I. S.; Kim, H. J.; Park, J. C.; Lee, S. Y. *Jpn. J. Appl. Phys., Part 1* **2002**, *41*, 820−825.
(26) Lashdaf, M.; Hatanpaa, T.; Krause, A. O. I.; Lahtinen, J.; Lindblad, M.; Tiitta, M. *Appl. Catal., A* **2003**, *241*, 51−63.
(27) Sun, H. J.; Kim, K. M.; Kim, Y. S.; Cho, K. J.; Park, K. S.; Lee, J. M.; Roh, J. S. *Jpn. J. Appl. Phys., Part 1* **2003**, *42*, 582−586.
(28) Sun, H. J.; Kim, Y. S.; Song, H. S.; Lee, J. M.; Roh, J. S.; Sohn, H. C. *Jpn. J. Appl. Phys., Part 1* **2004**, *43*, 1566−1570.
(29) Chi, Y.; Lee, F. J.; Liu, C.-S. U.S. Patent 6303809, 2001.
(30) Senzaki, Y.; Gladfelter, W. L.; McCormick, F. B. *Chem. Mater.* **1993**, *5*, 1715−1721.
(31) Senzaki, Y.; McCormick, F. B.; Gladfelter, W. L. *Chem. Mater.* **1992**, *4*, 747−749.
(32) Lai, Y. H.; Chen, Y. L.; Chi, Y.; Liu, C. S.; Carty, A. J.; Peng, S. M.; Lee, G. H. *J. Mater. Chem.* **2003**, *13*, 1999−2006.
(33) Smith, K. C.; Sun, Y. M.; Mettlach, N. R.; Hance, R. L.; White, J. M. *Thin Solid Films* **2000**, *376*, 73−81.
(34) Barreca, D.; Buchberger, A.; Daolio, S.; Depero, L. E.; Fabrizio, M.; Morandini, F.; Rizzi, G. A.; Sangaletti, L.; Tondello, E. *Langmuir* **1999**, *15*, 4537−4543.
(35) Choi, J.; Choi, Y.; Hong, J.; Tian, H.; Roh, J. S.; Kim, Y.; Chung, T. M.; Oh, Y. W.; Kim, C. G.; No, K. *Jpn. J. Appl. Phys., Part 1* **2002**, *41*, 6852−6856.
(36) McCormick, F. B.; Gladfelter, W. L.; Senzaki, Y. U.S. Patent 5372849, 1994.
(37) Yuan, Z.; Puddephatt, R. J.; Sayer, M. *Chem. Mater.* **1993**, *5*, 908−910.
(38) Sankar, J.; Sham, T. K.; Puddephatt, R. J. *J. Mater. Chem.* **1999**, *9*, 2439−2444.
(39) Chen, L.; Magtoto, N.; Ekstrom, B.; Kelber, J. *Thin Solid Films* **2000**, *376*, 115−123.
(40) Dey, S. K.; Goswami, J.; Bhaskar, S.; Cao, W.; Noh, W. C. *J. Vac. Sci. Technol. B* **2004**, *22*, L32−L34.
(41) Kwon, O. K.; Kim, J. H.; Park, H. S.; Kang, S. W. *J. Electrochem. Soc.* **2004**, *151*, G109−G112.
(42) Blackburn, J. M.; Long, D. P.; Cabanas, A.; Watkins, J. J. *Science* **2001**, *294*, 141−146.
(43) Watkins, J. J.; Blackburn, J. M.; McCarthy, T. J. *Chem. Mater.* **1999**, *11*, 213−215.
(44) Watkins, J. J.; McCarthy, T. J. U.S. Patent 5789027, 1998.
(45) Long, D. P.; Blackburn, J. M.; Watkins, J. J. *Adv. Mater.* **2000**, *12*, 913−915.
(46) Hunde, E. T.; Watkins, J. J. *Chem. Mater.* **2004**, *16*, 498−503.
(47) Fernandes, N. E.; Fisher, S. M.; Poshusta, J. C.; Vlachos, D. G.; Tsapatsis, M.; Watkins, J. J. *Chem. Mater.* **2001**, *13*, 2023−2031.
(48) Cabanas, A.; Shan, X. Y.; Watkins, J. J. *Chem. Mater.* **2003**, *15*, 2910−2916.
(49) Cabanas, A.; Blackburn, J. M.; Watkins, J. J. *Microelectron. Eng.* **2002**, *64*, 53−61.
(50) Blackburn, J. M.; Long, D. P.; Watkins, J. J. *Chem. Mater.* **2000**, *12*, 2625−2631.
(51) Ohde, H.; Kramer, S.; Moore, S.; Wai, C. M. *Chem. Mater.* **2004**, *16*, 4028−4031.
(52) Kondoh, E.; Kato, H. *Microelectron. Eng.* **2002**, *64*, 495−499.
(53) Kondoh, E. *Jpn. J. Appl. Phys., Part 1* **2004**, *43*, 3928−3933.
(54) Zong, Y. F.; Watkins, J. J. *Chem. Mater.* **2005**, *17*, 560−565.

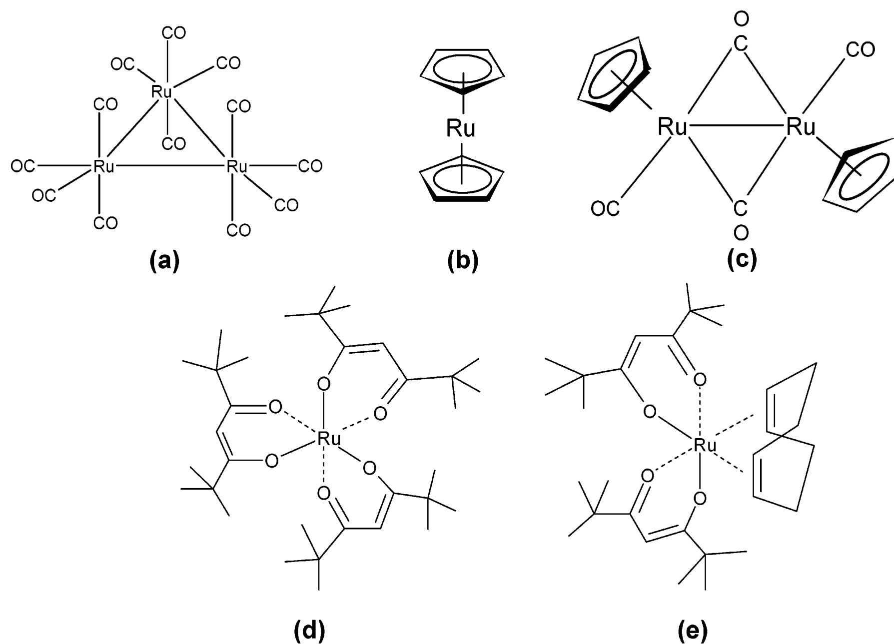

Figure 1. Ru precursors used in this study: (a) triruthenium dodecacarbonyl, (b) ruthenocene, (c) dicarbonyl cyclopentadiene ruthenium dimer, (d) tris-(2,2,6,6-tetramethyl heptane-3,5-dionato)ruthenium, and (e) bis(2,2,6,6-tetramethyl heptane-3,5-dionato)-1,5-cyclooctadienylruthenium.

$(CO)_{12}$, 99%), tris(2,2,6,6-tetramethyl-heptane-3,5-dionato)ruthenium ($Ru(tmhd)_3$, 99%) and bis(2,2,6,6-tetramethyl heptane-3,5-dionato)(1,5-cyclooctadiene)ruthenium ($Ru(tmhd)_2cod$, 99%) were obtained from Strem Chemicals and were used as received (Figure 1). Coleman grade CO_2 (99.99%), prepurified grade H_2 (99.99%), and prepurified grade N_2 (99.998%) were obtained from Merriam Graves. Flat silicon and tantalum-coated silicon wafers were donated by Novellus Systems, Inc. Etched tantalum-coated wafers were donated by Intel. All wafers were cut into squares of either 15 mm × 15 mm or 30 mm × 30 mm before film deposition.

SFD experiments were carried out in a 70 mL cold wall reactor containing a heated stage. Samples were secured on the stage and a known amount of precursor was added as solid. The vessel was then sealed and purged with N_2, while the wall temperature was brought to 60 °C. CO_2 was then added (11−15 MPa) and the vessel was left to equilibrate. H_2 was added to the vessel via a pressure drop from a 70 mL manifold. The amount of H_2 transferred was calculated from the pressure difference in the H_2 manifold and was in approximately 1000× excess. The pedestal heater was set to the endpoint temperature, and the reaction timer started once the stage temperature was within 5 °C of the set point. Initial heating profiles for the stage varied depending on the endpoint temperature: 150 °C was reached within 2 min, while heating to 300 °C required 3.5 min. Upon completion of the deposition experiment, the vessel was allowed to cool. The stage temperature dropped rapidly, typically more than 100 °C in less than a minute. The deposition was believed to be effectively terminated when the stage temperature fell below 200 °C. The deposition time was generally 30 min, but was reduced for several short, high-temperature depositions. Thermal decompositions were carried out using the procedure described above except that the addition of the H_2 was omitted.

X-ray photoelectron spectroscopy (XPS) was conducted using a Physical Instruments Quantum 2000 Scanning ESCA Microprobe. Scanning electron microscopy (SEM) was performed using a Joel 6320F Field Emission Microscope. Samples were cleaved by fracture after scoring with a diamond-tipped knife and mounted using silver paste onto an aluminum disk. Cross-sectional samples were mounted at 90° and a 5 nm gold coating was used to ensure conduction over the whole surface. Atomic force microscopy (AFM) was carried out using a Digital Instruments Dimension 3000 scanning probe microscope in contact mode with a SiN tip. X-ray diffraction (XRD) of the film was carried out using a Philips X-Pert diffractometer with a Cu Kα source. Film thicknesses were measured by profilometry using a Dektak 3 profilometer for films greater than 20 nm thickness and by AFM for thinner films. Sheet resistivities were calculated using thickness measurements and resistances were measured using a Jandel four-point probe. Adhesion was assessed using a scribe tape test. The test involves scoring the 10 mm × 10 mm film in a cross-hatched pattern (100 squares) followed by application and removal of a pressure-sensitive adhesive (PSA) by pulling at 90° to the surface. A sample was deemed to pass if no metal is transferred to the PSA after its removal. The scribe tape method is qualitative; however, it is a demanding test that is commonly employed to assess film adhesion.

Results and Discussion

A representative summary of experiments and results is provided in Table 1. The 30 min deposition time used in most of the experiments was chosen arbitrarily and the measured film thicknesses do not necessarily reflect the deposition kinetics. For example, a film grown at 275 °C for 30 min using triruthenium dodecacarbonyl was approximately twice the thickness of a film grown for 5 min at that same temperature, indicating that the precursor was likely consumed prior to completion of the 30 min experiment. All depositions were carried out at high excess of hydrogen and precise concentration was not believed to be a factor that influenced film quality or thickness. Moreover, the backside of the deposition stage is not fully insulated. Because the depositions are conducted in batch mode, deposition on the underside of the stage competes for available precursor. At elevated temperatures in particular, this competition will limit film thickness on the substrate.

The triruthenium dodecacarbonyl precursor system has been used previously in CVD investigations. Ruthenium exists in the zero oxidation state in the precursor, which decomposes readily, both thermally and in the presence of

Table 1. Representative Data for Ru Films Deposited in Supercritical Carbon Dioxide[a]

expt	precursor	substrate	temp (°C)	deposition time (min)	precursor (wt %)	hydrogen (wt %)	hydrogen excess	thickness (nm)	resistivity ($\mu\Omega$-cm)	adhesion
1	$Ru_3(CO)_{12}$	Si	250	30	0.22	0.59	870	32.8	22.2	fail
2	$Ru_3(CO)_{12}$	Si	275	5	0.11	0.46	1350	27.8	30.6	fail
3	$Ru_3(CO)_{12}$	Si	275	30	0.09	0.42	1460	51.1	29.5	fail
4	$Ru_3(CO)_{12}$	Si	300	/	0.12	0.49	1260	6.9	74.7	pass
5	$Ru_3(CO)_{12}$	Si	300	30	0.10	0.44	1460	57.1	23.6	fail
6	$Ru_3(CO)_{12}$	Ta	200	30	0.08	0.37	1420	23.9	51.8	pass
7	$Ru_3(CO)_{12}$	Ta	250	5	0.09	0.45	1550	23.2	38.4	pass
8	$Ru_3(CO)_{12}$	Ta	275	/	0.12	0.50	1400	9.1	17.6	pass
9	$Ru_3(CO)_{12}$	Ta	300	/	0.12	0.49	1260	13.4	22.8	pass
10	$Ru_3(CO)_{12}$	Si	175	30	0.09	0	0	0		
11	$Ru_3(CO)_{12}$	Si	225	30	0.09	0	0	56.7	1277	pass
12	$Ru_3(CO)_{12}$	Si	250	30	0.10	0	0	109.9	452.9	fail
13	$Ru_3(CO)_{12}$	Si	275	30	0.10	0	0	63.6	659.8	fail
14	$Ru(Cp)_2$	Si	300	30	0.42	0.50	140	0		
15	$Ru(Cp)_2$	Au	300	30	0.41	0.51	150	40.1	51.2	fail
16	$[Ru(CO)_2(Cp)]_2$	Si	225	30	0.09	0.38	900	71.1	1302	pass
17	$[Ru(CO)_2(Cp)]_2$	Si	250	30	0.11	0.40	840	33.4	111.9	pass
18	$[Ru(CO)_2(Cp)]_2$	Si	300	30	0.10	0.44	930	100.3	1675	pass
19	$Ru(tmhd)_3$	Si	175	30	0.53	0.54	330	27.8	120.7	fail
20	$Ru(tmhd)_3$	Si	200	30	0.54	0.45	270	55.8	82.3	fail
21	$Ru(tmhd)_3$	Si	250	30	0.06	0.50	2550	28.8	80.8	fail
22	$Ru(tmhd)_2cod$	Si	200	30	0.08	0.42	1520	30.6	109.3	pass
23	$Ru(tmhd)_2cod$	Si	225	30	0.07	0.34	1310	31.9	113.8	pass
24	$Ru(tmhd)_2cod$	Si	250	5	0.10	0.41	1200	37.0	98.4	pass
25	$Ru(tmhd)_2cod$	Si	250	30	0.10	0.38	1140	48.7	76.5	fail
26	$Ru(tmhd)_2cod$	Si	275	5	0.10	0.53	1570	48.5	55.6	fail
27	$Ru(tmhd)_2cod$	Ta	275	5	0.12	0.56	1330	31.5	19.0	fail
28	$Ru(tmhd)_2cod$	Ta	300	1	0.10	0.44	1270	23.7	31.7	pass

[a] Final reaction pressures ranged between 20 and 25 MPa. A reaction time represented by "/" indicates the stage was heated to the deposition temperature and then immediately allowed to cool. Adhesion was tested using a scribe tape test, as described in the text.

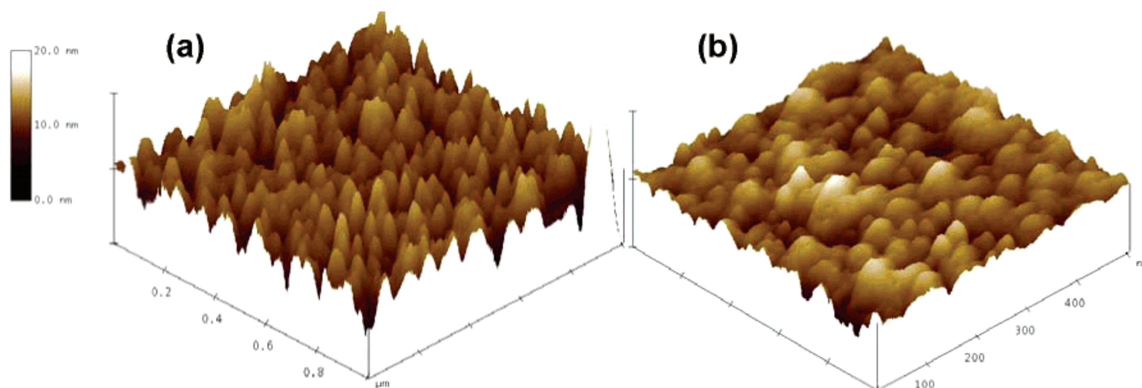

Figure 2. (a) Contact AFM image of a film surface grown using the $Ru_3(CO)_{12}$. This film was 28 nm thick and was grown at 275 °C over 5 min. (b) AFM image of a similar film (32 nm) grown from $Ru(tmhd)_2cod$ at 300 °C over 30 min. Precise roughness measurements were difficult to obtain due to tip damage from the extremely hard ruthenium surface. It was clear, however, that films grown from $Ru(tmhd)_2cod$ were smoother than those grown from the $Ru_3(CO)_{12}$. Recorded values of rms roughness of the films were 3.1 nm (a) and 1.8 nm (b). The differences in roughness are also observed in SEM.

hydrogen. However, CVD experiments using this precursor are generally unsuccessful due to low vapor pressure and low decomposition temperature.

$Ru_3(CO)_{12}$ has been reported to be soluble in CO_2.[55] SCF deposition, using this precursor, in the presence of hydrogen proceeded readily on the native oxide of silicon and on Ta films at temperatures between 200 and 300 °C. In all cases, high-quality, mirror-like films were grown. Thicknesses between 6.5 and 110 nm were obtained; however, the continuity of the films was compromised below 20 nm thickness, where island formation was evident. For the Ru films deposited using $Ru_3(CO)_{12}$, adhesion appears to be dependent on film thickness. Those films less than 25 nm exhibited strong adhesion, while those greater than 25 nm generally did not. This appears to be true regardless of the deposition temperature. The resistivity of films grown in the presence of hydrogen decreased with increasing film thickness as might be expected; values as low as 22 $\mu\Omega$-cm were measured for a 33 nm film. This compares favorably with films generated by other methods: for example, Wang et al. recorded values of 30 $\mu\Omega$-cm using CVD and Kwon et al. values of 15 $\mu\Omega$-cm with ALD.[15,41]

XPS analysis of a 57 nm film was consistent with pure ruthenium (Figure 3). Oxygen impurities were not detected and only spectral noise in the photoelectron region corresponding to oxygen was present (Figure 3 inset). Oxygen was also absent from the interfacial regions, where trace amounts would be expected due to the native oxide of silicon. Oxygen was consistently absent from the Si wafer interface

(55) Kreher, U.; Schebesta, S.; Walther, D. *Z. Anorg. Allg. Chem.* **1998**, *624*, 602−312.

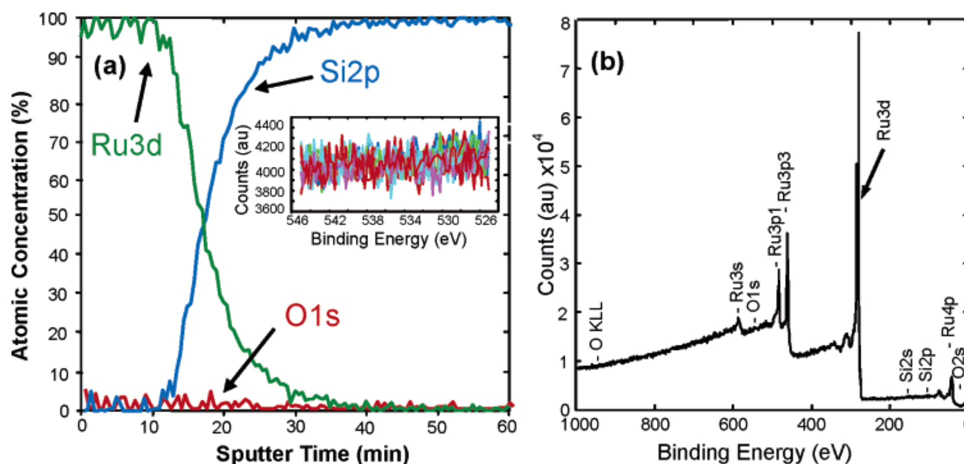

Figure 3. (a,b) XPS data of a film deposited using $Ru_3(CO)_{12}$ revealed little or no oxygen contamination. The film was grown at 300 °C over 30 min. The inset data is the oxygen region of the XPS data, indicating that the atomic concentration of oxygen was at the detection limit of the instrument. Absence of silicon in the survey spectrum indicates a uniform film with no pinholes.

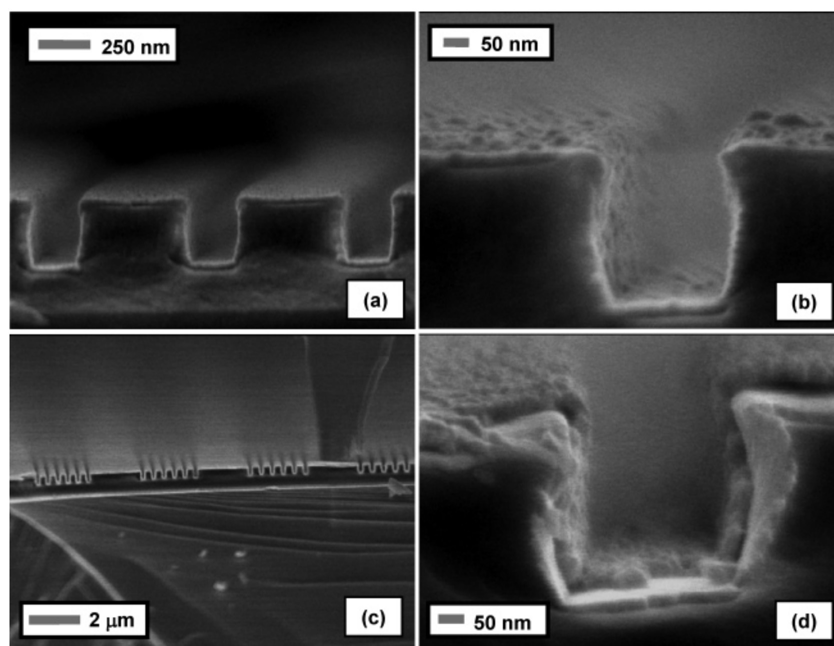

Figure 4. SEM images of conformal films deposited on Ta-coated wafers using $Ru_3(CO)_{12}$ at 300 °C (a,b) or $Ru(tmhd)_2cod$ at 275 °C (c,d).

for films grown from $Ru_3(CO)_{12}$ in the presence of hydrogen and temperatures above 275 °C. This was not observed in other precursor systems. Due to spectral overlap between carbon and the much stronger ruthenium peak, it was not possible to ascertain the carbon content in these or any other ruthenium films by XPS, directly. Analysis of the ratio of a Ru standard and Ru peaks measured above were indistinguishable; even though the signal received from Ru 3d was greater when compared to that of C 1s, this does not represent definitive proof of negligible carbon content. The absence of significant carbon may be inferred from the resistivity measurements as carbon impurities would significantly raise the resistance in the film above the measured values. AFM was carried out on a 28 nm thick film and revealed a continuous, well intergrown surface topology with an rms roughness of 3.1 nm (Figure 2). XRD results were consistent with the hexagonal structure of pure ruthenium (Figure 5). The ruthenium peaks were indexed using the DICVOL04[56,57] program (a = 2.7020 Å, c = 4.2723 Å) and found to be consistent with data for pure ruthenium (a = 2.7039 Å, c = 4.2817 Å).[58,59]

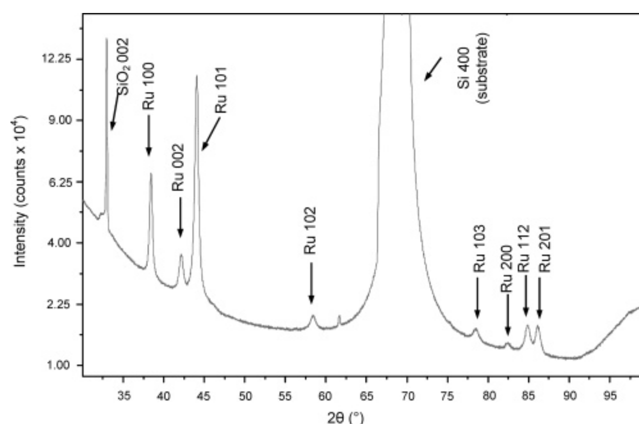

Figure 5. XRD for a film deposited using $Ru_3(CO)_{12}$ at 300 °C. The data suggest a hexagonal structure consistent with pure ruthenium on a silicon substrate. Ruthenium oxide impurities were not detected.

(56) Boultif, A.; Louer, D. *J. Appl. Crystallogr.* **2004**, *37*, 724−731.

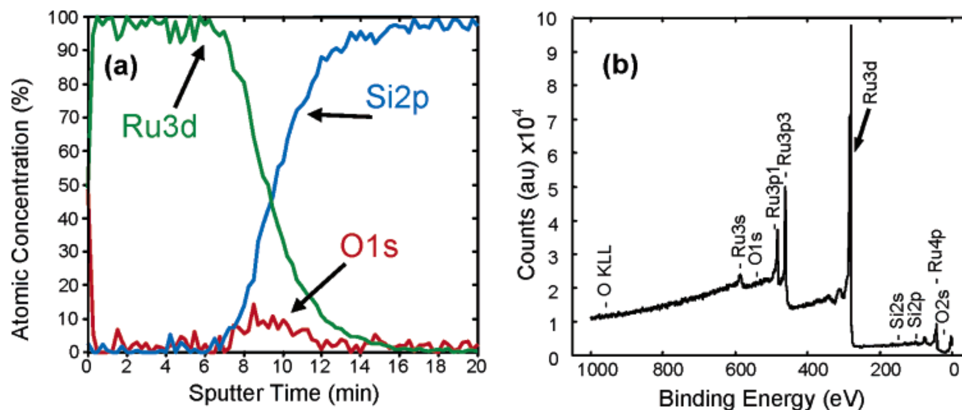

Figure 6. XPS data indicate that high-purity ruthenium films are deposited from $Ru(tmhd)_2cod$ at 300 °C. The presence of oxygen at the metal interface evident in the depth profile (a) was ascribed to the initial native oxide of silicon. Oxygen and silicon content of the film are at the detection limits as determined by high-resolution analysis of the O 1s (525−545 eV) and Ru 3d (277−297 eV) binding regions and by examination of a survey spectrum (b) taken within the film.

Growth of the films from triruthenium dodecacarbonyl by thermal rather than reduction driven deposition was also possible and yielded highly reflective films. However, noticeable differences in resistivities were measured. The thermally grown films were much less conducting than those grown by H_2-assisted deposition. Carbon contamination in Ru cannot be identified by XPS analysis; carbon content is inferred by the high resistivities shown in Table 1. It is therefore apparent that the use of a reductant was required for pure, highly conducting films. Deposition onto tantalum wafers produced thicker films in comparison to films grown onto the native oxide of silicon and under similar conditions. Lower resistivity was observed in these films and adhesion was also improved in the films deposited on the Ta surfaces relative to the native oxide.

Step coverage for Ru deposition via SFD is excellent. Figure 4a,b shows conformal deposition on a Ta-coated patterned wafer. The deposition was conducted for 5 min at 275 °C in the presence of hydrogen. The observed film roughness would be an issue for ultrathin interconnect barrier applications, but is less important for capacitor electrode structures.

We also attempted depositions using ruthenocene, which has been used in several CVD studies.[3−5] The precursor was chosen for use in supercritical carbon dioxide as it was expected to be considerably more soluble in CO_2 than the $Ru_3(CO)_{12}$ and is also similar in structure to metallocenes of Ni and Co that have been previously been used in SFD.[46] We found that depositions were not successful on Si and Ta wafers and no films were observed at temperatures below 300 °C. This is in contrast to the results of Kondoh who was able to grow conformal films using the ruthenocene precursor in a hot wall reactor.[53] Kondoh, however, used gold seed layers and higher deposition temperatures (350 °C). Our subsequent reproduction of Kodoh's results yielded films of ruthenium which grew more slowly than films grown with other precursors under similar conditions. Comparable CVD depositions occurred at higher temperatures of 300−500 °C.

The $[Ru(CO)_2Cp]_2$ dimer provided a ligand system that offers a potential compromise, improving solubility relative to $Ru_3(CO)_{12}$, while providing more efficient decomposition. Films grown from this precursor at temperatures between 225 and 300 °C were highly reflective and uniform. No deposition was observed without H_2 present as a reducing agent. Oxygen contamination could not be detected in the films by XPS, indicating successful removal of the carbonyl ligands. Precise control of the deposition, however, was problematic. Thicknesses were unpredictable and resistivities were higher than expected, indicating possible carbon contamination and/or poor film continuity. AFM analysis showed that the films grown using this precursor were extremely rough, far rougher than those grown from the carbonyl precursor (rms roughness 10−30 nm). A lack of interconnectivity between these larger grains likely contributes to the high film resistivities. Lack of control over the deposition and high film resistivity renders this precursor of limited interest for further study.

SFD using diketone-based ligand systems has been highly successful for other metal systems. Use of $Ru(tmhd)_3$, however, produced variable results. Films were deposited in the presence of hydrogen at temperatures between 175 and 250 °C (Table 1). The films were continuous and highly reflective, but exhibited poor adhesion for film thicknesses greater than 20 nm. AFM data revealed granular films that were well interconnected. Resistivities around 80 $\mu\Omega$-cm were recorded but these values rose sharply with decreasing film thickness due to the onset of island formation. This precursor system appears to deliver the necessary purity and conformality; however, the deposited films lack adequate adhesion.

The final precursor tested was $Ru(tmhd)_2cod$, which is similar to the $Ru(tmhd)_3$, except for the replacement of a tetramethylheptanedione ligand with cyclooctadiene. This precursor has been successfully used in oxygen-assisted CVD experiments.[40] SFD using this precursor yielded highly pure films. The XPS survey data taken after initial sputtering with Ar^+ indicated that oxygen contamination was not present in the bulk of the film, Figure 6. XPS sputter depth profiling, however, revealed that there is oxygen present at the Si/Ru

(57) Wiles, D. B.; Young, R. A. *J. Appl. Crystallogr.* **1981**, *14*, 149−151.
(58) www-mincryst; http://database.iem.ac.ru/mincryst/, accessed June 2005.
(59) Wyckoff, R. W. G.; 2 ed.; Interscience Publishers: 1963; Vol. 1, 8−11.

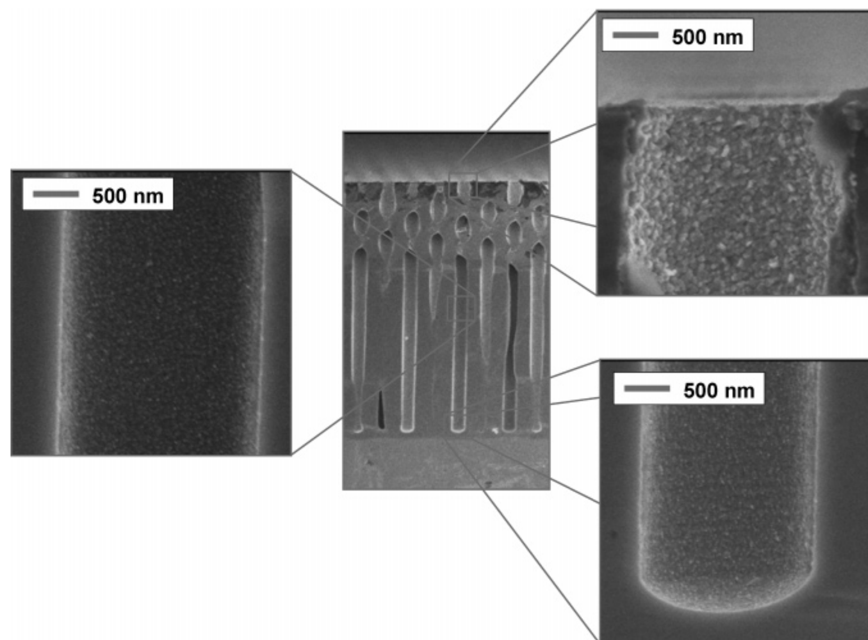

Figure 7. SEM image of an Ru film deposited within a 15:1 aspect ratio via. The film was grown from Ru(tmhd)$_2$cod at 250 °C.

interface, indicative of the native oxide of silicon. Film resistivity was as low as 19 $\mu\Omega$-cm, which was similar to the results for the triruthenium dodecacarbonyl carbonyl system. The films grown at lower temperatures appear to possess superior adhesion even when the film thickness is greater than 25 nm. XRD for a film grown at 300 °C reveals a hexagonal structure of pure ruthenium very similar to the result for $Ru_3(CO)_{12}$, shown in Figure 5. Film deposition was uniform across the wafer section used for SEM analysis, approximately 4 mm in length. AFM indicated that surface roughness for films deposited from Ru(tmhd)$_2$cod was lower than films deposited using $Ru_3(CO)_{12}$ (Figure 2b). An rms value of 1.8 nm was recorded for this film, which was grown at 275 °C. This is supported by SEM data which show conformal coverage of ruthenium over a trench structure. Step coverage was excellent and uniform over the patterned topography (Figure 4c,d). Improvement in roughness relative to the $Ru_3(CO)_{12}$ was also evident in the SEM images. A more challenging topography is shown in Figure 7 where good step coverage was achieved in a 30 μm deep hole with an aspect ratio of 15. Slightly greater film thickness is evident at the top of the hole, but this tapers rapidly to yield an even film over the majority of the feature. A third profile is shown in Figure 8, where a via structure was coated with a ruthenium film. The film conforms to the shape of the via in which it was originally grown and is either wholly retained or wholly removed on fracturing, indicating a cohesive, well interconnected film. Conformal depositions in deep vias are attractive for the preparation of 3D capacitor electrodes.

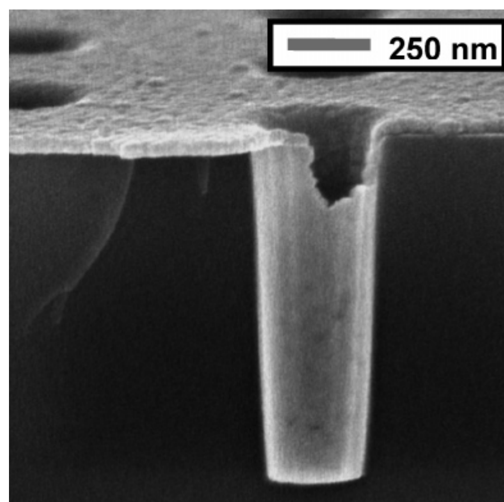

Figure 8. A ruthenium film grown at 275 °C remains intact during fracturing for sample preparation. The unsupported outer edge of the film remains interconnected and adherent to the base of the via structure.

Conclusions

Ru depositions proceed readily in supercritical CO_2. Promising results were obtained using $Ru_3(CO)_{12}$ and Ru(tmhd)$_2$cod, both of which could be used to deposit pure, conformal, low-resistivity films over challenging topographies. The films deposited in this study are too thick for use in current damascene architectures as barrier systems. However, the deposition of bottom electrodes in capacitor structures using these systems is attractive.

Acknowledgment. Funding for this work was provided by the National Science Foundation (CTS-0245002) and Novellus Systems, Inc. Instruments supported by the Materials Research Science and Engineering Center at the University of Massachusetts were used for analysis.

CM060142D